

# Few-Shot Learning for Industrial Defect Detection on Novel Scanning Electron Microscopy Datasets

Anonymous Full Paper  
Submission 34

## Abstract

Industrial Defect Detection (IDD) involves identifying defects in different products through the analysis of manufacturing data. Over recent years convolutional neural networks (CNN) have become the preferred method to reliably solve this task, though a lack of labeled data has been a key challenge for supervised methods that rely on CNNs. Few-Shot Learning (FSL) offers a promising solution by enabling models to learn tasks from only a small number of labeled examples. However, it shifts the need for large labeled datasets to the pre-training stage, raising questions about how well these models generalize to new domains, such as different imaging modalities. Therefore, this study evaluates state-of-the-art FSL methods, trained on public optical datasets, for their effectiveness in IDD when tested on scanning electron microscopy (SEM) images. To facilitate benchmarking, this article also introduces three distinct SEM datasets for defect detection purposes. Through this assessment the study is able to identify strengths, challenges, and potential areas of improvement to motivate further research.

**Keywords:** Industrial defect detection, convolutional neural networks, few-shot learning, scanning electron microscopy images.

## 1 Introduction

Recent developments in the field of computer vision have significantly accelerated the creation and training of automated systems to inspect industrial products at several stages of manufacturing. Inspection and analysis of such data not only enable quality control on the production line but also the detection of key areas to potentially improve existing manufacturing processes [1, 2]. Industrial defect detection (IDD) presents a task to detect anomalies in industrial manufacturing data that manifest themselves in modalities such as optical inspection (grayscale or color), X-ray imaging, or electron microscopy images of components, parts, assembly, and tiny semiconductor structures. In this domain, the current state of the art presents itself in supervised methods that rely on Convolutional Neural Networks (CNNs) and large amounts of task-specific labeled data [3, 4]. Since reviewing and manually labeling images for every task is necessary but time-

and labor-intensive task in the case for supervised methods, models that can quickly learn a new task from just a few labeled examples are particularly valuable. This motivates the use of few-shot learning (FSL) for IDD, where methods aim to adapt to previously unseen tasks using only a small number of annotated images. As FSL methods have been shown to be competitive with standard supervised models in a classification setting [5] and semantic segmentation for IDD [2], this paper uses FSL methods in a classification setting to detect industrial defects. However, FSL does not eliminate the need for large labeled datasets; it merely shifts the problem from training a task-specific model to training a more general model capable of handling a wide range of tasks. In practice, this often involves relying on publicly available, large-scale optical image datasets for pre-training. These datasets must capture the underlying characteristics of the target tasks to be effective, yet while there is an abundance of data for some modalities, such as natural images, there is very limited publicly available data for others, such as defect detection in SEM images. In this work, we aim to develop an understanding of how well FSL methods can be adapted to defect detection from an industrial perspective by benchmarking these methods on real-world scanning electron microscope (SEM) images provided to by [COMPANY NAME OBSCURED FOR BLIND REVIEW]. In tandem, this would also provide an outlook on how well models are able to generalize when trained on optical images but benchmarked on SEM images. The contributions of this paper can be summarized as follows:

- Publication of three scanning electron microscopy datasets for the purposes of industrial defect detection at the courtesy of [COMPANY NAME OBSCURED FOR BLIND REVIEW].
- Proposal of a new evaluation framework to evaluate few-shot learning methods in the context of industrial applications for defect detection.
- Benchmarking insights on how few-shot learning methods work when trained on publicly available data and applied on real-life industrial data from a different imaging modality.

## 092 2 Methods

### 093 2.1 Few-Shot Learning Problem Formalization

094 The main aim of few-shot learning (FSL) is to extract  
095 transferable knowledge from an auxiliary data set  
096  $A$  to adapt to a new unseen task  $T$  with a small  
097 amount of labeled samples. For example, given a  
098 dataset  $D$ , it's split into  $D_{train}$ ,  $D_{val}$ , and  $D_{test}$  to  
099 train and evaluate FSL methods. Each split is class  
100 disjointed; meaning, that it is possible to define sets  
101 of classes  $C_{train}$ ,  $C_{val}$ , and  $C_{test}$  exclusively belong  
102 to their own split.  $D_{train}$  is utilized as  $A$ , which is  
103 a class-rich split and is assumed to be within the  
104 same domain as  $D_{val}$  and  $D_{test}$ . A task  $T$  is defined  
105 by two sets: a labeled support set and an unlabeled  
106 query set. The support set  $S$  contains  $N$  classes  
107 with  $K$  samples per class, which is why few-shot  
108 learning tasks are commonly described as N-way-K-  
109 shot in classification settings. To evaluate a model's  
110 ability to learn from limited samples, such tasks  $T$   
111 are randomly sampled from  $D_{val}$  and  $D_{test}$ . A query  
112 set  $Q$  is comprised of  $K$  samples per class from the  
113 same label space as  $S$  and is utilized to evaluate the  
114 performance of a given method for a specific task.  
115

### 116 2.2 Few-Shot Learning Methods Evaluated in This Study

117 This paper evaluates a total of six few-shot learning  
118 methods (mentioned in Table 1.) which span two  
119 major categories: non-episodic and episodic meth-  
120 ods. Non-episodic methods are similar to transfer  
121 learning methods in which a model is pre-trained on  
122 the auxiliary set and then fine-tuned during infer-  
123 ence on the given support set [6]. Episodic methods  
124 are further divided into two subtypes: meta-learning  
125 and metric learning. Meta-learning aims to learn  
126 with small gradient steps to quickly adapt to an  
127 unseen new task. Metric learning methods adapt  
128 to a new task by comparing the distances between  
129 images from the support and query set images [6].  
130 The methods evaluated in this paper are as fol-  
131 lows: Baseline is a non-episodic transfer learning  
132 approach; the model is pre-trained on auxiliary data  
133 and then fine-tuned on target tasks [7]. SKD (Gen-0)  
134 is another non-episodic method that employs self-  
135 supervision with data augmentation to learn a broad  
136 classification manifold [8]. Among episodic meta-  
137 learning methods, MAML trains models to rapidly  
138 adapt to new tasks using only a few gradient steps  
139 through meta-learning [9]. BOIL also uses episodic  
140 meta-learning but differs by updating only the fea-  
141 ture extractor during the inner-loop updates [10].  
142 In episodic metric learning, ProtoNet classifies by  
143 computing distances to prototype representations of  
144 each class [11], while RENet enhances metric learn-  
145 ing with self-correlation and correlational attention  
146 to capture rich semantic relationships between query  
147

and support sets.

### 2.3 Implementation Details

The methods discussed above are implemented by Li  
et al. [6] in an open-source project called LibFewShot,  
which aims to facilitate research within the few-shot  
learning (FSL) paradigm. Built in PyTorch [12],  
LibFewShot provides re-implementations of 18 state-  
of-the-art FSL methods with multiple backbones  
and a flexible yet reproducible framework to per-  
form comparative experiments. Following common  
practice [6, 11, 13], all images in this study (training  
and evaluation) are resized to 84 x 84 pixels and  
normalized as preprocessing, and the LibFewShot  
training procedure is followed where the performance  
on the validation set is monitored to save the best  
performing model. Although methods commonly use  
Conv64F, ResNet-12, and ResNet-18 as backbones  
[6, 10, 14], for this study, the simplest backbone  
(Conv64F) is selected based on time feasibility and  
computational resources available. The architecture  
of Conv64F includes four identical blocks where each  
block is composed of a convolutional layer with 64  
3x3 filters, a batch normalization layer, a ReLU /  
LeakyReLU layer and an optional max-pooling layer  
[6, 11]. Each method has a preferred optimizer and  
hyperparameters, LibFewShot provides suggestive  
configurations, which are followed for this study.  
Following common practice [9, 11], for each method  
mentioned, models are trained in the 1-shot and  
5-shot scenarios. Then the models are evaluated in  
1-shot, 5-shot, 10-shot, and 20-shot scenarios.

Table 1. Methods evaluated in this study.

Method	Category	Subtype	Reference
Baseline	Non-Episodic	-	[7]
SKD (Gen-0)	Non-Episodic	-	[8]
MAML	Episodic	Meta-Learning	[9]
BOIL	Episodic	Meta-Learning	[10]
ProtoNet	Episodic	Metric Learning	[11]
RENet	Episodic	Metric Learning	[13]

### 2.4 Metric and Evaluation Framework

#### 2.4.1 Metric

As a key challenge in defect detection tasks is the  
high imbalance between classes, where defect sam-  
ples tend to be rarer than non-defect ones, accu-  
racy as a metric can be misleading due to the  
over-representation of the majority class in the test  
dataset [15]. To illustrate this issue, consider a test  
dataset with 990 non-defect images and 10 images  
with defects. If a given classifier predicts all 1000  
images of the test set to be non-defect, it would au-  
tomatically achieve an accuracy of 99%, which fails  
to capture the failure of the classifier to predict the  
minority class entirely. To account for a classifier's  
ability to predict the majority and minority classes,

195 this study adopts balanced accuracy as the reported  
 196 metric, which can be described as the average recall  
 197 for all classes from a dataset (eq.1). This ensures  
 198 that each class is represented equally regardless of  
 199 its prevalence in the dataset [15]. For a multi-class  
 200 classification problem with  $N$  distinct classes, the  
 201 balanced accuracy is defined as:

$$202 \quad \text{Balanced Accuracy} = \frac{1}{N} \sum_{i=1}^N \frac{TP_i}{TP_i + FN_i}, \quad (1)$$

203 where  $TP_i$  and  $FN_i$  are the numbers of true posi-  
 204 tive and false negative predictions, respectively, for  
 205 the  $i$ th label.

### 206 2.4.2 Evaluation Framework

207 LibFewShot provides a standardized framework for  
 208 evaluating FSL methods. It assesses models by sam-  
 209 pling 3,000 balanced tasks from a data split and  
 210 reporting the mean accuracy with a 95% confidence  
 211 interval [6]. This standardized process enables con-  
 212 sistent benchmarking in academic research; however,  
 213 because classes are randomly sampled, tasks may  
 214 include unrelated classes. As this study is interested  
 215 in measuring the performance of models for indus-  
 216 trial applications on specific tasks, the evaluation  
 217 strategy was updated accordingly in the following  
 218 way: Instead of sampling multiple tasks from a  
 219 dataset, the entire evaluation dataset is turned into  
 220 one task, where a support set is defined of  $K$ -shots  
 221 from  $N$ -classes from the dataset (illustrated in Fig.  
 222 1), and the remainder of it is considered a query  
 223 set. This enables us to estimate the approximate  
 224 performance of a model for a given dataset when  
 225 using a few-shot learning method. To capture the  
 226 true range of results over multiple support sets, the  
 227 updated evaluation process described in this paper  
 228 is repeated 50 times with randomized support sets,  
 229 and the mean of balanced accuracy and the 95% con-  
 230 fidence interval are reported. The evaluation process  
 231 is conducted on all test datasets sets individually to  
 232 record accuracy per dataset. Although these fifty  
 233 evaluations conducted are significantly lower than  
 234 the standard of 3000 evaluations in LibFewShot,  
 235 query sets are commonly limited to 15 images per  
 236 class in a task during regular evaluation [11], while  
 237 query sets in this study are significantly larger. This  
 238 allows the study to leverage more data to provide rep-  
 239 resentative results while addressing computational  
 240 constraints.

## 241 3 Experiments & Results

### 242 3.1 Datasets

243 For conducting experiments, the Industrial 5i  
 244 dataset [1] is utilized as the auxiliary and validation  
 245 set containing 80% and 20% of classes, respectively.  
 246 The Industrial 5i dataset (Fig. 6), introduced by

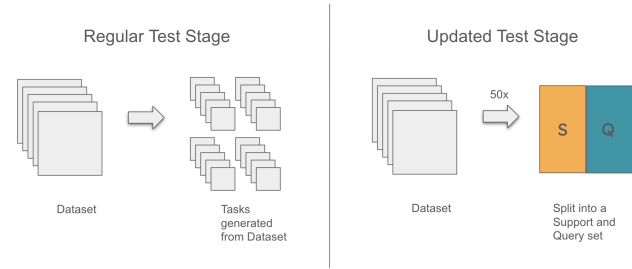


Figure 1. Updated evaluation framework for this study illustrated.

247 [1] was originally proposed for a  $K$ -shot image seg-  
 248 mentation task and comprises common industrial  
 249 datasets such as MVTEC-AD [16], KolektorSDD [3],  
 250 etc. Each product has a positive class (non-defect)  
 251 and negative class (defect) and a corresponding bi-  
 252 nary mask as a label for semantic segmentation.  
 253 The data set is converted into a classification task to  
 254 align with the objective of the project and then used  
 255 for training and validation. With 20 products and 2  
 256 classes per product, the dataset is recreated with 40  
 257 total classes and to prevent data leakage between  
 258 classes of the same product, the train, and valida-  
 259 tion splits are randomly allocated distinct products  
 260 instead of classes. The product-wise split is followed  
 261 to ensure a model learns to distinguish between good  
 262 and defective classes within the same dataset.

### 263 3.1.1 Scanning Electron Microscope 264 Datasets

265 The three test datasets are produced by and pub-  
 266 lished at the courtesy of [COMPANY NAME OB-  
 267 SCURED FOR BLIND REVIEW]. Each dataset rep-  
 268 represents a unique pattern created by electron-beam  
 269 lithography, with bright areas being the silicon wafer  
 270 trench floor and unexposed PMMA (polymethyl  
 271 methacrylate) resist being the dark area. The data  
 272 sets are captured with an SEM detector biased to  
 273 collect as many electrons as possible, resulting in  
 274 additional brightness around any shape edge present  
 275 in the data set. These data sets differ from each  
 276 other in a key characteristic. 'Trench' was created  
 277 specifically to test models with artificially added  
 278 defects that are positionally consistent from image  
 279 to image. 'Lines & Spaces' and 'Josephson Junc-  
 280 tion' were created for meteorological studies and  
 281 the labels are added through manual annotation of  
 282 naturally occurring defects. Figures 3, 4, and 5 show  
 283 samples of each class present within the data sets,  
 284 and the class distributions of the evaluation datasets  
 285 are illustrated in Fig. 2. The descriptive statistics  
 286 for each split of the dataset are mentioned in Table  
 287 2.

### 288 3.2 Results

289 For each method mentioned, a model is trained in  
 290 the 5-way-1-shot and 5-way-5-shot scenarios. They

**Table 2.** Descriptive Statistics of Data Splits.

Split	# Unique Classes	# Images
Train/Auxiliary	30	16,070
Validation	10	1,111
Test	Trench: 6, JJ: 3, L&S: 2	Trench: 1,200, JJ: 1,000, L&S: 1,000

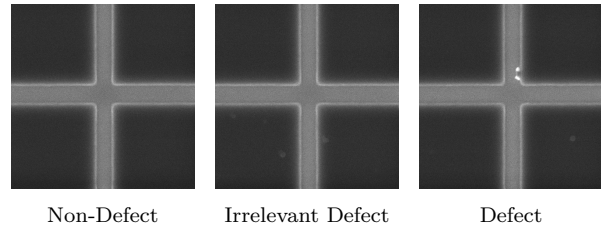
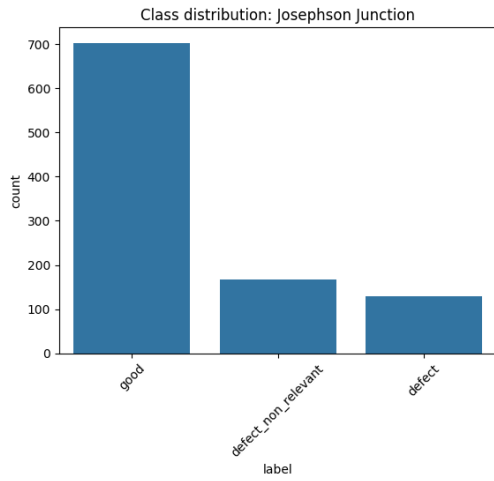


**Figure 3.** Classes from the Josephson Junction dataset.

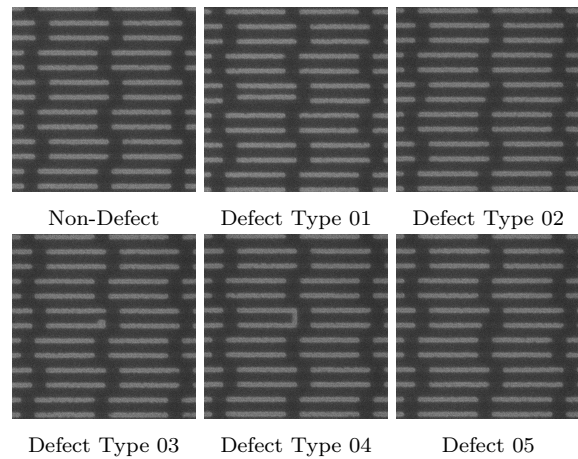
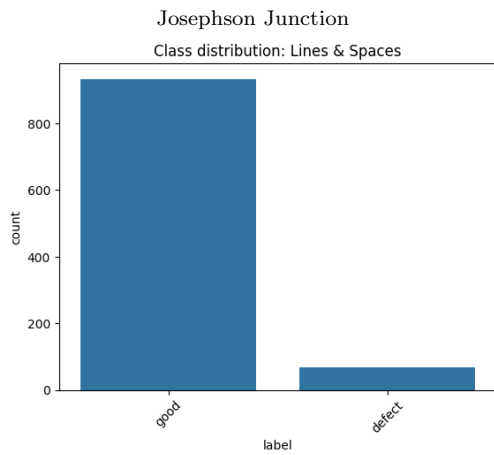


**Figure 4.** Classes from the Trench dataset.

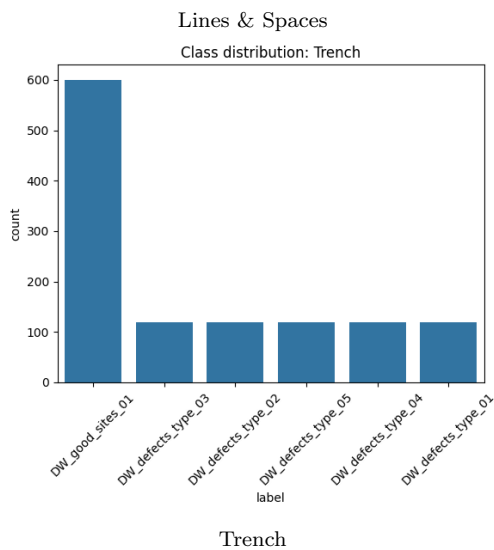


**Figure 5.** Classes from the Lines & Spaces dataset.

**Figure 2.** Class distributions of the evaluation datasets.

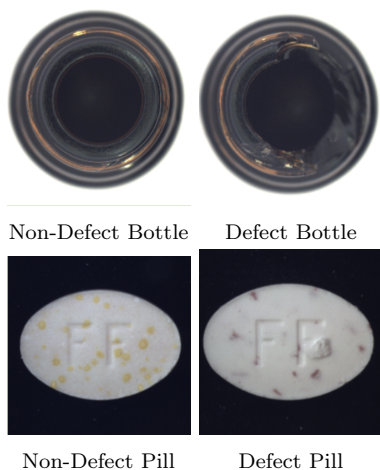


**Figure 6.** Examples of products from Industrial 5i.

are then evaluated in the 1-shot, 5-shot, 10-shot, and 20-shot scenarios with each dataset. The reported metrics as shown in Tables 3, 4, and 5 indicate that the FSL methods successfully adapt to the 6-Way Trench dataset with the best-performing model achieving  $96.63\% \pm 0.26\%$  balanced accuracy in the 20-shot scenario. On the other hand, the methods fail to adapt to the 3-Way Josephson Junction (JJ), and 2-Way Lines & Spaces (L&S) datasets in all scenarios, with the best-performing models achieving  $52.41\% \pm 1.79\%$  and  $38.89\% \pm 1.70\%$  balanced accuracies in the 20-shot scenario respectively. A model randomly assigning labels, where the accuracy it obtains can be described as  $100/N$ -Way, would achieve 16.67% balanced accuracy on Trench, 33.34% balanced accuracy on Josephson Junction, and 50% balanced accuracy on Lines & Spaces. Comparing these to the best-performing trained models on JJ and L&S signifies ineffective learning and motivates an investigation into the potential reasons behind the poor performance. Furthermore, for the 50 evaluations in each scenario, an average confusion matrix (ACM) is computed to display the general behaviors of a model and common errors in a specific dataset. The ACM generated for the best-performing model per dataset in Fig 7.

### 3.3 Discussion

The Trench dataset yields a much stronger model performance than the JJ and L&S datasets. Given that Trench is specifically engineered to test defect detection algorithms, it can mean that Trench does not have the same natural noise and characteristics as present in the JJ and L&S datasets, which are derived from real products. This synthetic nature of the Trench dataset could explain its better performance. Looking at the performance on the other datasets, misclassification patterns observed in JJ and L&S may stem from several factors. First, the pre-processed image size of  $84 \times 84$  pixels used for

training and evaluation could have limited the granularity of visual information, as downsizing often degrades performance and introduces label noise [17, 18]. Second, the use of a small, randomly initialized backbone like Conv-64F, rather than a larger pre-trained model such as ResNet-18, could have further hindered performance. Finally, randomness in tasks when sampling for classes in the meta-learning process may have created poorly balanced tasks, for example, those with only defective or non-defective images, or with images from entirely different products. This could cause the model to focus on product classification rather than defect detection, diverging from the intended objective.

## 4 Conclusion

This article evaluates multiple few-shot learning methods for industrial defect detection on real-world scanning electron microscopy (SEM) images. Through testing, we were able to highlight the best performing methods; specifically *Baseline*, and identify potential problems in using the methods where the models did not perform effectively on the Josephson Junction and the Lines & Spaces dataset but perform comparatively well on the Trench dataset. The underlying random sampling technique and/or characteristic differences in the datasets may explain this variability in performance, although this requires further investigation.

## Acknowledgments

This work was supported by [EMPLOYEE OBSCURED FOR BLIND REVIEW] at [COMPANY OBSCURED FOR BLIND REVIEW], who created the Trench, Josephson Junction, and Lines & Spaces datasets. Furthermore, a significant portion of the research and writing presented in this paper is based on the master’s thesis of the [CORRESPONDING AUTHOR].

## References

- [1] X. Shi, S. Zhang, M. Cheng, L. He, X. Tang, and Z. Cui. “Few-Shot Semantic Segmentation for Industrial Defect Recognition”. In: *Computers in Industry* 148 (June 2023). ISSN: 0166-3615. DOI: [10.1016/j.compind.2023.103901](https://doi.org/10.1016/j.compind.2023.103901).
- [2] G. Xie, J. Wang, J. Liu, J. Lyu, Y. Liu, C. Wang, F. Zheng, and Y. Jin. “IM-IAD: Industrial Image Anomaly Detection Benchmark in Manufacturing”. In: *IEEE Transactions on Cybernetics* (2024), pp. 1–14. ISSN: 2168-2267. DOI: [10.1109/TCYB.2024.3357213](https://doi.org/10.1109/TCYB.2024.3357213). URL: <https://ieeexplore.ieee.org/document/10443076/>.

**Table 3.** Few-shot classification accuracies of the Conv-64F backbone on the Trench dataset are reported with mean balanced accuracy and 95% confidence intervals. A random classifier would achieve 16.66%. The best model is shown in bold, and the second-best in red. Meta-learning models are constrained by their training scenario (e.g., a 5-Way model can only be evaluated in 5-Way settings or less). To allow evaluation on the 6-Way Trench dataset, meta-learning models are instead trained in 6-Way scenarios\*.

Model	6-Way-1-Shot	6-Way-5-Shot	6-Way-10-Shot	6-Way-20-Shot
Baseline 5-Way-1-Shot	47.59% ± 1.11%	<b>74.03% ± 2.29%</b>	64.61% ± 4.42%	59.50% ± 2.90%
Baseline 5-Way-5-Shot	<b>54.97% ± 1.72%</b>	<b>85.64% ± 0.87%</b>	<b>92.9% ± 0.40%</b>	<b>96.63% ± 0.26%</b>
SKD Gen 0 5-Way-1-Shot	<b>53.25% ± 1.76%</b>	65.9% ± 1.33%	<b>72.85% ± 0.76%</b>	<b>78.02% ± 0.50%</b>
SKD Gen 0 5-Way-5-Shot	48.65% ± 2.41%	65.07% ± 1.18%	71.48% ± 0.82%	77.37% ± 0.57%
MAML 6-Way-1-Shot*	35.95% ± 1.63%	55.89% ± 2.48%	60.44% ± 1.74%	63.30% ± 1.40%
MAML 6-Way-5-Shot*	27.52% ± 1.00%	49.35% ± 2.47%	56.26% ± 1.56%	58.97% ± 1.12%
BOIL 6-Way-1-Shot*	45.32% ± 2.01%	58.99% ± 1.53%	62.02% ± 0.85%	62.66% ± 0.61%
BOIL 6-Way-5-Shot*	47.21% ± 1.82%	62.32% ± 1.35%	66.21% ± 0.87%	69.21% ± 0.80%
ProtoNet 5-Way-1-Shot	49.75% ± 2.77%	58.71% ± 1.72%	63.95% ± 1.45%	67.19% ± 0.75%
ProtoNet 5-Way-5-Shot	39.22% ± 1.58%	51.21% ± 1.77%	54.65% ± 1.62%	56.53% ± 1.35%
RENet 5-Way-1-Shot	47.00% ± 2.48%	61.36% ± 1.47%	64.81% ± 1.05%	68.71% ± 0.75%
RENet 5-Way-5-Shot	41.19% ± 2.68%	52.70% ± 1.42%	53.35% ± 0.55%	54.50% ± 0.36%

**Table 4.** Few-shot classification accuracies of the Conv-64F backbone on the Lines & Spaces dataset are reported with mean balanced accuracy and 95% confidence intervals. A random classifier would achieve 16.66%. The best model is shown in bold, and the second-best in red. Meta-learning models are constrained by their training scenario (e.g., a 5-Way model can only be evaluated in 5-Way settings or less). To allow evaluation on the 6-Way Trench dataset, meta-learning models are instead trained in 6-Way scenarios\*.

Model	2-Way-1-Shot	2-Way-5-Shot	2-Way-10-Shot	2-Way-20-Shot
Baseline 5-Way-1-Shot	<b>50.40% ± 5.91%</b>	50.78% ± 3.08%	<b>51.27% ± 2.46%</b>	50.6% ± 1.63%
Baseline 5-Way-5-Shot	50.02% ± 6.94%	<b>51.81% ± 3.06%</b>	51.19% ± 2.17%	<b>52.41% ± 1.79%</b>
SKD Gen 0 5-Way-1-Shot	50.07% ± 4.62%	50.92% ± 2.69%	50.92% ± 2.83%	<b>51.33% ± 1.84%</b>
SKD Gen 0 5-Way-5-Shot	50.23% ± 4.79%	50.07% ± 3.36%	49.26% ± 2.75%	49.83% ± 2.37%
MAML 6-Way-1-Shot*	49.69% ± 3.00%	<b>51.31% ± 5.00%</b>	<b>51.29% ± 3.08%</b>	50.84% ± 2.05%
MAML 6-Way-5-Shot*	<b>51.67% ± 3.53%</b>	50.50% ± 3.94%	51.10% ± 2.55%	50.74% ± 2.02%
BOIL 6-Way-1-Shot*	49.98% ± 4.03%	50.86% ± 3.41%	50.69% ± 2.98%	50.57% ± 2.83%
BOIL 6-Way-5-Shot*	50.08% ± 3.91%	50.53% ± 3.01%	50.90% ± 2.64%	51.08% ± 2.81%
ProtoNet 5-Way-1-Shot	49.88% ± 6.57%	49.88% ± 4.70%	48.95% ± 3.39%	50.17% ± 3.64%
ProtoNet 5-Way-5-Shot	50.16% ± 6.08%	49.16% ± 2.75%	50.82% ± 2.50%	50.60% ± 2.46%
RENet 5-Way-1-Shot	49.87% ± 6.50%	49.72% ± 4.38%	50.10% ± 3.55%	49.60% ± 3.49%
RENet 5-Way-5-Shot	49.77% ± 5.51%	50.57% ± 4.20%	50.36% ± 3.78%	50.28% ± 3.07%

382 [3] D. Tabernik, S. Šela, J. Skvarč, and D. Skočaj. pp. 6979–6998. ISSN: 1366588X. DOI: [10.1080/00207543.2024.2316279](https://doi.org/10.1080/00207543.2024.2316279). 399

383 “Segmentation-Based Deep-Learning Approach 400

384 for Surface-Defect Detection”. In: *Journal of* 401

385 *Intelligent Manufacturing* 31.3 (Mar. 2019), 402

386 pp. 759–776. DOI: [10.1007/s10845-019-01476-x](https://doi.org/10.1007/s10845-019-01476-x). URL: <https://doi.org/10.1007/s10845-019-01476-x>. 403

387 404

388 405

389 [4] I. Konovalenko, P. Maruschak, J. Brezinová, 406

390 J. Viňáš, and J. Brezina. “Steel surface defect 407

391 classification using deep residual neural 408

392 network”. In: *Metals* 10.6 (June 2020), p. 846. 409

393 ISSN: 2075-4701. DOI: [10.3390/met10060846](https://doi.org/10.3390/met10060846). 410

394 [5] P. Zajec, J. M. Rožanec, S. Theodoropoulos, 411

395 M. Fontul, E. Koehorst, B. Fortuna, and D. 412

396 Mladenčić. “Few-shot learning for defect 413

397 detection in manufacturing”. In: *International* 414

398 *Journal of Production Research* 62 (19 2024), 415

[6] W. Li, Z. Wang, X. Yang, C. Dong, P. Tian, T. Qin, J. Huo, Y. Shi, L. Wang, Y. Gao, and J. Luo. “LibFewShot: A Comprehensive Library for Few-Shot Learning”. In: *IEEE Transactions on Pattern Analysis and Machine Intelligence* 45 (12 Dec. 2023), pp. 14938–14955. ISSN: 19393539. DOI: [10.1109/TPAMI.2023.3312125](https://doi.org/10.1109/TPAMI.2023.3312125).

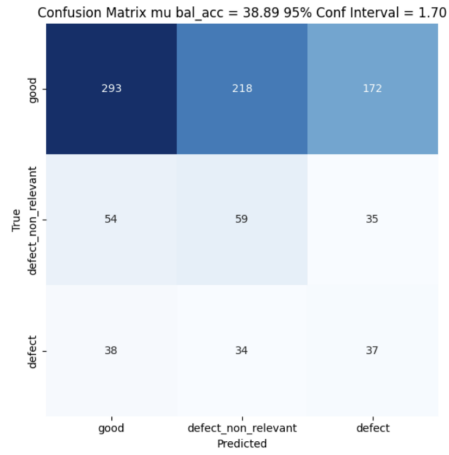
[7] W.-Y. Chen, Y.-C. Liu, Z. Kira, Y.-C. F. Wang, and J.-B. Huang. “A Closer Look at Few-shot Classification”. In: (Apr. 2019). URL: <http://arxiv.org/abs/1904.04232>.

[8] J. Rajasegaran, S. Khan, M. Hayat, F. S. Khan, and M. Shah. “Self-supervised Knowledge Distillation for Few-shot Learning”. In:

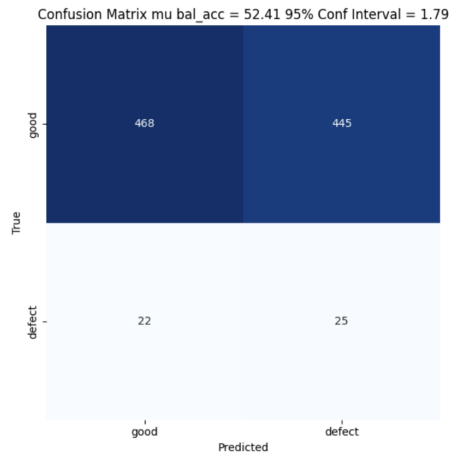
**Table 5.** Few-shot classification accuracies of the Conv-64F backbone on the Josephson Junction dataset are reported with mean balanced accuracy and 95% confidence intervals. A random classifier would achieve 16.66%. The best model is shown in bold, and the second-best in red. Meta-learning models are constrained by their training scenario (e.g., a 5-Way model can only be evaluated in 5-Way settings or less). To allow evaluation on the 6-Way Trench dataset, meta-learning models are instead trained in 6-Way scenarios\*.

Model	3-Way-1-Shot	3-Way-5-Shot	3-Way-10-Shot	3-Way-20-Shot
Baseline 5-Way-1-Shot	<b>34.75% ± 3.23%</b>	33.91% ± 1.45%	33.74% ± 2.64%	33.33% ± 0.00%
Baseline 5-Way-5-Shot	33.45% ± 4.03%	35.83% ± 2.44%	35.87% ± 1.06%	33.41% ± 0.04%
SKD Gen 0 5-Way-1-Shot	33.72% ± 2.92%	34.85% ± 1.97%	35.18% ± 1.49%	36.77% ± 1.37%
SKD Gen 0 5-Way-5-Shot	33.56% ± 3.43%	34.90% ± 2.40%	36.40% ± 1.77%	37.59% ± 1.71%
MAML 6-Way-1-Shot*	33.48% ± 5.54%	33.31% ± 7.80%	33.31% ± 7.35%	33.37% ± 8.05%
MAML 6-Way-5-Shot*	33.53% ± 3.59%	33.77% ± 5.86%	34.06% ± 6.26%	34.00% ± 5.93%
BOIL 6-Way-1-Shot*	34.14% ± 2.34%	35.13% ± 2.12%	<b>36.97% ± 2.61%</b>	37.02% ± 2.25%
BOIL 6-Way-5-Shot*	34.60% ± 2.40%	35.18% ± 2.32%	36.10% ± 2.59%	37.93% ± 2.50%
ProtoNet 5-Way-1-Shot	<b>34.72% ± 3.97%</b>	<b>36.80% ± 1.75%</b>	36.59% ± 1.59%	<b>38.55% ± 1.32%</b>
ProtoNet 5-Way-5-Shot	33.89% ± 2.79%	<b>36.85% ± 1.98%</b>	<b>37.42% ± 1.81%</b>	<b>38.89% ± 1.70%</b>
RENet 5-Way-1-Shot	34.25% ± 2.97%	34.60% ± 2.56%	34.41% ± 2.35%	36.61% ± 2.28%
RENet 5-Way-5-Shot	34.19% ± 2.53%	35.25% ± 1.96%	35.22% ± 1.65%	36.46% ± 1.75%

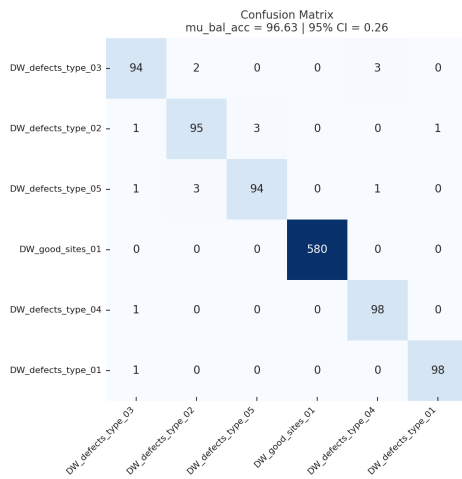
416 (June 2020). URL: [http://arxiv.org/abs/](http://arxiv.org/abs/2006.09785) [16] P. Bergmann, M. Fauser, D. Sattlegger, and C. 452  
417 [2006.09785](http://arxiv.org/abs/2006.09785). Steger. “MVTec AD-A Comprehensive Real- 453  
418 [9] C. Finn, P. Abbeel, and S. Levine. “Model- World Dataset for Unsupervised Anomaly 454  
419 Agnostic Meta-Learning for Fast Adaptation Detection”. In: (2019). URL: [www.mi.imati.cnr.](http://www.mi.imati.cnr.it/ettore/NanoTWICE/) 455  
420 of Deep Networks”. In: (Mar. 2017). URL: <http://arxiv.org/abs/1703.03400>. it/ettore/NanoTWICE/. 456  
421 [10] J. Oh, H. Yoo, C. Kim, and S.-Y. Yun. “BOIL: 457  
422 Towards Representation Change for Few-shot Impact of Image Size on Accuracy and Generaliza- 458  
423 Learning”. In: (Aug. 2020). URL: [http:// tion of Convolutional Neural Networks”. In: 459  
424 \[arxiv.org/abs/2008.08882\]\(http://arxiv.org/abs/2008.08882\). \*IJRAR19SP012 International Journal of Re- 460  
425 search and Analytical Reviews\* \(2019\). ISSN: 2349-5138. URL: \[www.ijrar.org\]\(http://www.ijrar.org\). 461  
426 \[11\] J. Snell, K. Swersky, and T. R. Zemel. “Proto- 462  
427 typical Networks for Few-shot Learning”. In: \[17\] M. Balaji, J. J. Luke, and R. Joseph. “Impact 457  
428 \(2017\). of Image Size on Accuracy and Generaliza- 458  
429 \[12\] A. Paszke, S. Gross, F. Massa, A. Lerer, J. tion of Convolutional Neural Networks”. In: 459  
430 Bradbury, G. Chanan, T. Killeen, Z. Lin, N. \*IJRAR19SP012 International Journal of Re- 460  
431 Gimelshein, L. Antiga, A. Desmaison, A. Köpf, search and Analytical Reviews\* \(2019\). ISSN: 461  
432 E. Yang, Z. DeVito, M. Raison, A. Tejani, S. 2349-5138. URL: \[www.ijrar.org\]\(http://www.ijrar.org\). 462  
433 Chalamkurthy, B. Steiner, L. Fang, J. Bai, and \[18\] V. Thambawita, I. Strümke, S. A. Hicks, P. 463  
434 S. Chintala. “PyTorch: An Imperative Style, Halvorsen, S. Parasa, and M. A. Riegler. “Im- 464  
435 High-Performance Deep Learning Library”. In: pact of image resolution on deep learning per- 465  
436 \(Dec. 2019\). URL: \[http://arxiv.org/abs/ formance in endoscopy image classification: 466  
437 1912.01703\]\(http://arxiv.org/abs/1912.01703\). An experimental study using a large dataset 467  
438 \[13\] D. Kang, H. Kwon, J. Min, and M. Cho. “Re- of endoscopic images”. In: \*Diagnostics\* 11 \(12 468  
439 lational Embedding for Few-Shot Classifica- Dec. 2021\). ISSN: 20754418. DOI: \[10.3390/\]\(https://doi.org/10.3390/diagnostics11122183\) 469  
440 tion”. In: \(Aug. 2021\). URL: \[http://arxiv. diagnostics11122183\]\(http://arxiv.org/abs/2108.09666\). 470  
441 \[org/abs/2108.09666\]\(http://arxiv.org/abs/2108.09666\).  
442 \[14\] Y. Song, T. Wang, P. Cai, S. K. Mondal, and  
443 J. P. Sahoo. “A Comprehensive Survey of Few-  
444 shot Learning: Evolution, Applications, Chal-  
445 lenges, and Opportunities”. In: \*ACM Comput-\*  
446 \*ing Surveys\* 55 \(13s July 2023\). ISSN: 15577341.  
447 DOI: \[10.1145/3582688\]\(https://doi.org/10.1145/3582688\).  
448 \[15\] J. S. Akosa. “Predictive Accuracy: A Mislead-  
449 ing Performance Measure for Highly Imbal-  
450 anced Data”. In: \*Proceedings of the SAS Global\*  
451 \*Forum\*. 2017.](http://arxiv.org/abs/2008.08882)



JJ



Lines & Spaces



Trench

Figure 7. Average confusion matrices of the best-performing model over 50 evaluation loops for each evaluation dataset.